

## Beyond Thermodynamics: Drug Binding Kinetics Could Influence Epidermal Growth Factor Signaling

Mayank Goyal, Michael Rizzo, Frank Schumacher, and  
Chung F. Wong\*

*Department of Chemistry and Biochemistry and the Center for  
Nanoscience, University of Missouri—Saint Louis, One University  
Boulevard, St. Louis, Missouri 63121*

*Received July 1, 2009*

**Abstract:** We modeled the kinetics of drug binding to protein kinases in the EGF signaling pathway relevant to non-small-cell lung cancer and found that binding kinetics could influence therapeutic potential, that fast binding kinetics was advantageous for most targets with a couple of exceptions, that targeting some protein kinases could enhance rather than attenuate the pathway, and that IC<sub>50</sub> could be sensitive to the kinetic parameters of drug binding.

Computer-aided drug design has mostly focused on considering binding strength or thermodynamics rather than kinetics. Yet there is already evidence that drug binding kinetics can also play a role. In a recent paper, Tummino and Copeland proposed that the residence time, rather than the binding affinity, determined the therapeutic potential of drug candidates.<sup>1</sup> They defined the residence time to be the inverse of  $k_{\text{off}}$ .

One study supporting this proposal concerned the design of peptide mimics to bind to the extracellular domain of the receptor tyrosine kinase human epidermal growth factor receptor 2 (HER2), a protein kinase in the same family as epidermal growth factor receptor (EGFR<sup>a</sup>).<sup>2</sup> In this work, the authors found that the desired cellular interference correlated better with the dissociation constant than with the binding affinity of the peptide mimics. Another example came from studies correlating the response of T cells with the types of MHC/peptide complexes with which they interacted. Whether the presented peptide by MHC was an agonist, partial agonist, antagonist, or one that did not trigger any T-cell response appeared to correlate with the duration of interaction between a T cell and an MHC/peptide complex.<sup>3–8</sup>

On the other hand, some studies found that  $k_{\text{on}}$ , rather than  $k_{\text{off}}$ , associated better with therapeutic potential. For example, Wu et al. showed that  $k_{\text{on}}$  of engineered antibodies linked better with the ability of the antibodies to neutralize the respiratory syncytial virus.<sup>9</sup>

To gain further insights into the role of drug-binding kinetics in drug discovery, we performed kinetic modeling on the epidermal growth factor (EGF) signaling pathway,

which is overly active in non-small-cell lung cancer, for example. Modeling has the advantage that it can be used to study theoretical compounds that may be difficult to make experimentally to help test a concept of drug design. For example, it is not easy to synthesize compounds with exactly the same binding affinity but different rate constants of drug–receptor association and dissociation to examine whether kinetics, in addition to thermodynamics, can be an important factor to consider in drug discovery. However, one can do this easily with a kinetic model.

In kinetic modeling, it is also useful to examine a larger pathway instead of only analyzing the impact of a drug candidate on its direct target. In this work, we studied the effects of applying theoretical drugs to different protein kinases in the EGF signaling pathway constructed previously by Wang et al.<sup>10</sup> We modified their pathway only slightly to include drug interactions. Figure 1 shows an example in which a drug is applied to the EGF-EGFR dimer denoted by (EGF:EGFR)<sub>2</sub>.

In order to study whether drug-binding kinetics could attenuate the production of the doubly phosphorylated form of MAP kinase (ERK-PP depicted in Figure 1) differently, we prepared theoretical drugs with exactly the same binding affinity ( $K_1$ ) to its protein kinase target but with different kinetic constants of binding ( $k_a$ ) and unbinding ( $k_d$ ) such that  $K_1 = k_d/k_a$  remained constant. If these drugs with exactly the same binding affinity  $K_1$  affected the activity of ERK-PP differently, one could conclude that binding kinetics indeed played a role in drug design. (We monitored the concentration of ERK-PP because its level of activity is believed to control cell proliferation.)

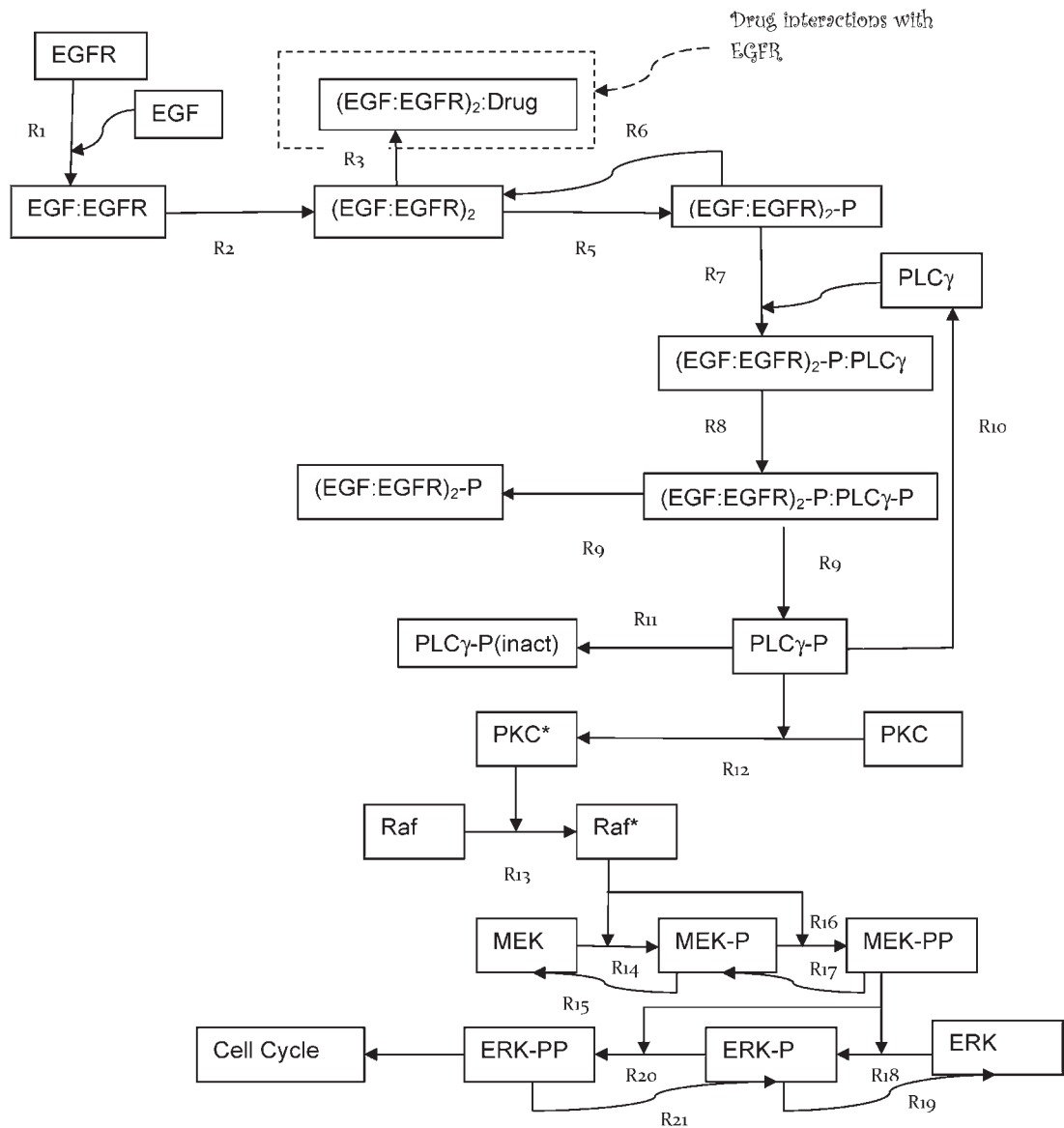
We performed kinetics modeling by using Copasi 4.5 (Build 30).<sup>11</sup> The model consisted of 22 molecules and involved solving 22 coupled differential equations. We used the same rate laws, kinetic constants, and initial concentrations as in Wang et al.'s work<sup>10</sup> except when we modeled an overactivated EGF-EGFR dimer or when we mimicked an overexpression of EGFR. On the other hand, because our model introduced drug binding, we modified one kinetic equation accordingly and added one equation for drug binding (step R<sub>3</sub> in Figure 1). The equations and parameters of the kinetic model are reported in Tables S1 and S2 of Supporting Information.

Figure 2 gives an example of the time course of the concentration of ERK-PP. The concentration rose to a maximum before decaying to zero. In this study, we monitored the change in the maximum concentration when different theoretical drugs were applied in order to calculate percent inhibition of ERK-PP, which was obtained by using the maximum concentration of ERK-PP before and after a drug was applied.

Table 1 shows that binding kinetics did affect ERK-PP production when we applied theoretical drugs with different kinetic, but same thermodynamic, parameters to the EGF-EGFR dimer. When we used a drug concentration of 1 nM (equaled to  $K_1$ ), there was no inhibition. But as we increased the concentration to 100 nM, appreciable inhibition appeared and the degree of inhibition depended on binding kinetics. Percent inhibition was low at slow binding kinetics but

\*To whom correspondence should be addressed. Phone: 314-516-5318. Fax: 314-516-5342. E-mail: wongch@umsl.edu.

<sup>a</sup>Abbreviations: EGF, epidermal growth factor; EGFR, epidermal growth factor receptor; PLC $\gamma$ , phospholipase c  $\gamma$ ; PKC, protein kinase C; Raf, MAP kinase kinase kinase; MEK, MAP kinase kinase; ERK, MAP kinase.



**Figure 1.** Pathway model for studying the influence of drug-binding kinetics on EGF signaling in non-small-cell lung cancer. A:B represents a complex between A and B. A-P denotes the phosphorylated form of A, and A-PP represents the doubly phosphorylated form of A. A\* indicates the activated form of A. Note: The single-direction arrows do not imply all reactions are unidirectional; some represent reversible reactions.

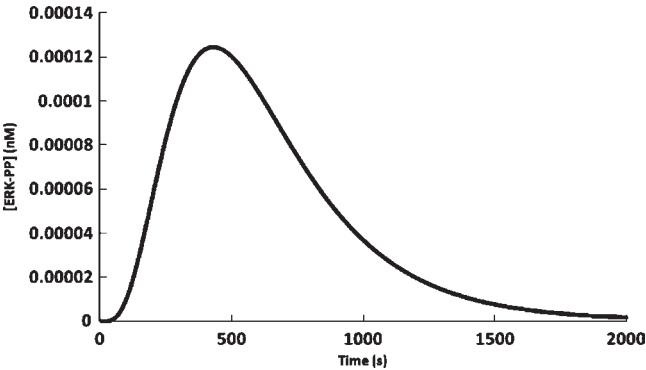


**Figure 2.** Time evolution of the concentration of ERK-PP as a function of time. A concentration of 10 nM of a theoretical drug, with  $K_1 = 1$  nM, was applied to  $(\text{EGF:EGFR})_2$  shown in Figure 1. The starting concentrations of EGF and EGFR were 132.5 and 80 nM, respectively. The maximum concentration was used to compute percent inhibition in this study.

**Table 1.** Inhibition of ERK-PP as a Function of Kinetic Parameters of Drug Binding<sup>a</sup>

$k_d$ ( $s^{-1}$ )	% inhibition			
	[drug] = 1 nM	[drug] = 10 nM	[drug] = 100 nM	[drug] = 100 nM
0.0001	0.0008	0.0032	0.1953	1.9255
0.001	0.0008	0.0145	10.8051	13.0047
0.01	0.0008	0.0209	43.2716	45.3306
0.1	0.0008	0.0185	43.8325	45.3210
1	0.0008	0.0193	43.8399	45.3202
10	0.0008	0.0193	43.8389	45.3202

<sup>a</sup>Theoretical drugs with different kinetic parameters and doses were applied to the EGF-EGFR dimer in the pathway shown in Figure 1. The starting concentrations of EGF and EGFR were 132.5 and 80 nM, respectively. The binding constant of the drugs to the dimer was fixed at  $K_1 = 1$  nM.  $k_d$  was the dissociation rate constant for the drug-receptor complexes. Results in the last column were obtained by using a truncated pathway in which only steps up to  $R_5$  in Figure 1 were included.

approached a maximum value with faster binding kinetics (note that as we increased the dissociation constant  $k_d$ , the

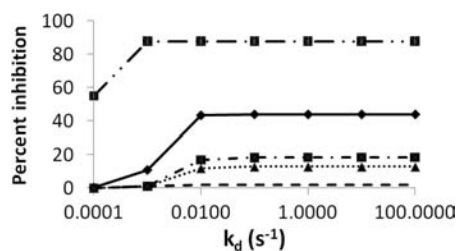


**Figure 3.** Percent inhibition versus drug–receptor dissociation rate constant  $k_d$ . The reference simulation (solid line) started with  $[EGFR] = 80$  nM,  $[EGF] = 132.5$  nM, and 100 nM drug with  $K_1 = 1$  nM applied to EGFR. Dashed line,  $K_1$  of the drug increased to 10 nM; dot-dashed line, starting concentration of EGFR increased by a factor of 10–800 nM; dot-dot-dashed line, concentration of EGFR decreased to 1 nM; dotted line, forward rate constant in step  $R_5$  in Figure 1 increased by 20 times;  $K_i$  of drug decreased to 0.1 nM.

association constant increased accordingly to keep  $K_1$  constant). The last column in Table 1 gives the results for a truncated pathway in which only steps  $R_1$ – $R_5$  in Figure 1 were included. The purpose of this computational experiment was to examine whether a simpler assay could predict the behavior of a more complex assay including more downstream steps. We found that this truncated pathway gave similar results as the larger pathway in Figure 1. The percent inhibition was nearly the same for the full and truncated pathways. (For the truncated pathway, we monitored the concentration of (EGF:EGFR)-P in Figure 1 instead of ERK-PP.)

Figure 3 shows similar qualitative dependence of percent inhibition on  $k_d$  when we decreased the binding affinity ( $K_1$ ) of the drug to the EGF-EGFR dimer by a factor of 10, when we decreased the concentration of EGFR to 1 nM, when we increased the concentration of EGFR by a factor of 10 to mimic an overexpression of the protein, and when we increased the rate constant of the phosphorylation of the EGF-EGFR dimer by 20 times to mimic an overactivated protein resulting from a diseased mutation, for example. (In this last case, we used a higher-affinity drug, with  $K_1 = 0.1$  nM, in order to obtain observable percent inhibition.)

Although applying drugs to most protein kinases in this pathway gave similar qualitative dependence of percent inhibition on  $k_d$  as those shown in Figure 3, there were exceptions. For example, when we applied a drug to the activated form of Raf, denoted by Raf\* in Figure 1, we observed that the percent inhibition peaked at an intermediate  $k_d$  approximately around  $1 \times 10^{-3} \text{ s}^{-1}$  and decreased afterward, instead of increasing monotonically with  $k_d$  to an asymptotic value as in the cases illustrated in Figure 3 (Figure 4). On the other hand, applying drug to the unactivated form of Raf showed the common behavior discussed earlier. The larger percent inhibition observed for the unactivated form of Raf also suggested that targeting the unactivated form of Raf might be more effective in attenuating ERK-PP production than targeting the activated form, according to this kinetic model.

Figure 5 shows yet another behavior when we applied drugs to the three different forms of MAP kinase kinase. Applying a drug to the unphosphorylated form, MEK, increased the production of ERK-PP rather than attenuating it. On the other hand, applying drugs to the singly or doubly phosphorylated forms of MEK reduced ERK-PP production.

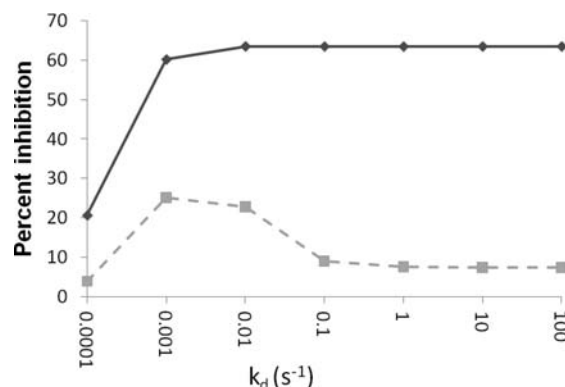


**Figure 4.** Percent inhibition of ERK-PP when 100 nM drug was applied to Raf (solid line) or Raf\* (dashed line). The forward rate constant of step  $R_5$  in Figure 1 was increased by a factor of 20 to mimic an overactivated EGF-EGFR dimer.

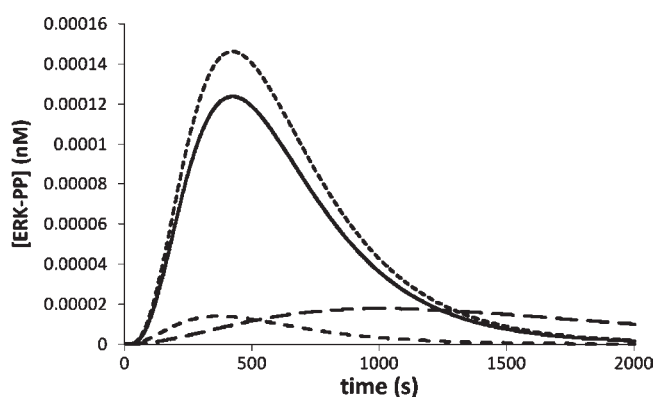


**Figure 5.** Applying drug to MEK elevated the production of ERK-PP rather than decreasing it (shortest dashed line). Solid line represents the reference state when no drug was applied. On the other hand, applying drugs to the singly and doubly phosphorylated forms of MAP kinase kinase attenuated the production of ERK-PP (the two plots with longer dashed lines). A concentration of 10 nM drug, with  $K_1 = 1$  nM, was used in each case.

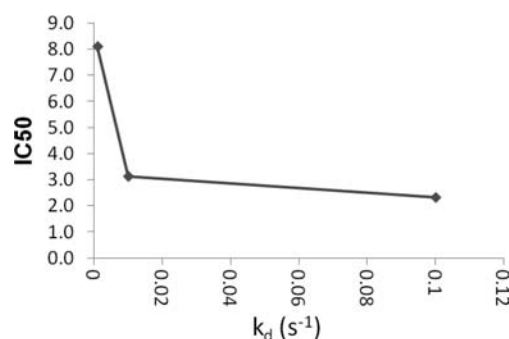


**Figure 6.**  $IC_{50}$  as a function of drug–receptor dissociation rate constant for MEK-P.  $K_1 = 1$  nM, and the forward rate constant for step  $R_5$  in Figure 1 was increased by a factor of 20 to mimic an overactivated EGF-EGFR dimer.

With the singly phosphorylated form of MAP kinase kinase, MEK-P, as an example, Figure 6 shows that  $IC_{50}$  obtained from a kinetic assay could depend on the kinetic constants of drug binding. The  $IC_{50}$  varied by about a factor of 4 for the range of  $k_d$  covered in the figure. Computational drug designers need to be aware of this, as they often compare

computed binding affinity) a thermodynamic rather than a kinetic quantity) with experimental  $\ln(\text{IC}_{50})$ .

In summary, our kinetic modeling of drug interference with protein kinases in the EGF signaling pathway showed that drug-binding kinetics could play a role in attenuating this pathway. Thus, tuning the kinetic parameters of drug binding can also be important in drug discovery. Although fast-binding kinetics seemed to be favored for most protein kinase targets in this pathway, there were exceptions. In the case of activated Raf, drug with intermediate kinetic constants appeared best. On the other hand, we found that applying a drug to a protein kinase such as the unphosphorylated form of MEK could activate rather than attenuate signaling. In addition, we found that  $\text{IC}_{50}$  could depend on drug binding kinetics when measured by kinetic assays. Although the reliability of our predictions on EGF signaling depends on how well this kinetic model reflects reality, the principles that drug-binding kinetics can play a role in drug discovery should be general. As kinetic models are continually being refined to fit experimental observations for specific pathways and networks, these models can play an important role in guiding drug discovery.

**Acknowledgment.** This research is supported in part by the National Institutes of Health.

**Supporting Information Available:** Tables S1 and S2 listing the species, rate laws, and kinetic parameters used in the pathway model based on the work of Wang et al.<sup>10</sup> This material is available free of charge via the Internet at <http://pubs.acs.org>.

## References

- (1) Tummino, P. J.; Copeland, R. A. Residence time of receptor-ligand complexes and its effect on biological function. *Biochemistry* **2008**, *47*, 5481–5492.
- (2) Berezov, A.; Zhang, H. T.; Greene, M. I.; Murali, R. Disabling erbB receptors with rationally designed exocyclic mimetics of antibodies: structure–function analysis. *J. Med. Chem.* **2001**, *44*, 2565–2574.
- (3) van der Merwe, P. A.; Davis, S. J. Molecular interactions mediating T cell antigen recognition. *Annu. Rev. Immunol.* **2003**, *21*, 659–684.
- (4) Germain, R. N.; Stefanova, I. The dynamics of T cell receptor signaling: complex orchestration and the key roles of tempo and cooperation. *Annu. Rev. Immunol.* **1999**, *17*, 467–522.
- (5) Davis, M. M.; Boniface, J. J.; Reich, Z.; Lyons, D.; Hampl, J.; Arden, B.; Chien, Y. Ligand recognition by alpha beta T cell receptors. *Annu. Rev. Immunol.* **1998**, *16*, 523–544.
- (6) Lyons, D. S.; Lieberman, S. A.; Hampl, J.; Boniface, J. J.; Chien, Y.; Berg, L. J.; Davis, M. M. A TCR binds to antagonist ligands with lower affinities and faster dissociation rates than to agonists. *Immunity* **1996**, *5*, 53–61.
- (7) Matsui, K.; Boniface, J. J.; Steffner, P.; Reay, P. A.; Davis, M. M. Kinetics of T-cell receptor binding to peptide/I-Ek complexes: correlation of the dissociation rate with T-cell responsiveness. *Proc. Natl. Acad. Sci. U.S.A.* **1994**, *91*, 12862–12866.
- (8) Savage, P. A.; Boniface, J. J.; Davis, M. M. A kinetic basis for T cell receptor repertoire selection during an immune response. *Immunity* **1999**, *10*, 485–492.
- (9) Wu, H.; Pfarr, D. S.; Tang, Y.; An, L. L.; Patel, N. K.; Watkins, J. D.; Huse, W. D.; Kiener, P. A.; Young, J. F. Ultra-potent antibodies against respiratory syncytial virus: effects of binding kinetics and binding valence on viral neutralization. *J. Mol. Biol.* **2005**, *350*, 126–144.
- (10) Wang, Z.; Zhang, L.; Sagotsky, J.; Deisboeck, T. S. Simulating non-small cell lung cancer with a multiscale agent-based model. *Theor. Biol. Med. Modell.* **2007**, *4*, 50.
- (11) Hoops, S.; Sahle, S.; Gauges, R.; Lee, C.; Pahle, J.; Simus, N.; Singhal, M.; Xu, L.; Mendes, P.; Kummer, U. COPASI—a Complex PAtchway SIMulator. *Bioinformatics* **2006**, *22*, 3067–3074.